Virus scaffolds

An Engineered Virus as a Scaffold for Three-Dimensional Self-Assembly on the Nanoscale**

Amy Szuchmacher Blum, Carissa M. Soto, Charmaine D. Wilson, Tina L. Brower, Steven K. Pollack, Terence L. Schull, Anju Chatterji, Tianwei Lin, John E. Johnson, Christian Amsinck, Paul Franzon, Ranganathan Shashidhar, and Banahalli R. Ratna**

Significant challenges exist in assembling and interconnecting the building blocks of a nanoscale device and being able to electronically address or measure responses at the molecular level. Self-assembly is one of the few practical strategies for making ensembles of nanostructures and will therefore be an essential part of nanotechnology.[1] In order to generate complex structures through self-assembly, it is essential to develop methods by which different components in solution can come together in an ordered fashion. One approach to achieve ordered self-assembly on the nanoscale is to use biomolecules such as DNA as scaffolds for directed assembly because of the specificity and versatility they provide.[2–4] Although several groups have demonstrated the usefulness of this approach, building ordered three-dimensional (3D) structures with DNA is difficult, because of the 1D nature of the scaffold.[3,5,6] Using viruses as nanoscale scaffolds for devices offers the promise of exquisite control

[*] Dr. A. S. Blum, Dr. C. M. Soto, Dr. T. L. Brower, Dr. S. K. Pollack, Dr. T. L. Schull, Dr. B. R. Ratna
Center for Bio/Molecular Science and Engineering
Naval Research Laboratory
4555 Overlook Avenue SW, Washington, DC 20375 (USA)
Fax: (+1) 202-404-3043
E-mail: amyblum@cbmse.nrl.navy.mil
ratna@nrl.navy.mil

C. D. Wilson
Geo-Centers, Inc.
Newton, MA 02459 (USA)

Dr. A. Chatterji, Prof. T. Lin, Prof. J. E. Johnson
Department of Molecular Biology
The Scripps Research Institute
10550 North Torrey Pines Road, La Jolla, CA 92037 (USA)

C. Amsinck, Prof. P. Franzon
Department of Electrical and Computer Engineering,
North Carolina State University, Raleigh, NC 27695 (USA)

Dr. R. Shashidhar
Geo-Centers, Inc.
4301 North Fairfax Drive, Suite 200, Room 248,
Arlington, VA 22203 (USA)

[**] Research support by the Defense Advanced Research Projects Agency is gratefully acknowledged. T.L.B. thanks the National Research Council for fellowship support.

Supporting information for this article is available on the WWW under http://www.small-journal.com or from the author.

  DOI: 10.1002/smll.200500021

of positioning on the nanoscale,[7,8] by using a particle that can either interface with lithographically defined structures, or undergo further self-assembly into extended structures by itself.[9,10] As a test case for proving the efficacy of this approach, we built 3D conductive molecular networks using cowpea mosaic virus (CPMV) as a scaffold.

CPMV is an icosahedral particle made of 60 copies of a protein subunit, with a spherically averaged diameter of 30 nm (Figure 1a). Its structure has been determined by X-ray crystallography to a resolution of 2.8 Å.[11] CPMV has been genetically engineered, resulting in the production of a large number of mutants.[12,13] Its icosahedral symmetry allows the generation of specific patterns of functional residues, which provide a means to assemble complex structures with high spatial specificity on the nanometer scale. In its natural state, CPMV contains no thiol-containing cysteine residues on the capsid exterior. We have genetically engineered CPMV to present cysteine residues at selected positions, which allow us to anchor gold nanoparticles that are subsequently interconnected by molecular wires to create a 3D conducting network on the nanoscale. The properties of the network can be changed by altering the position and hence the pattern of cysteine residues on the capsid surface.

The current work utilizes two different CPMV mutants, designated EF and DM. The EF mutant has a single cysteine (Figure 1b) inserted into the protein subunit as a GGCGG loop,[14] while the DM mutant (Figure 1c) has two cysteines inserted per subunit, replacing alanine and glutamic acid residues at positions 235 and 2319, respectively. Gold nanoparticles were bound to these engineered cysteine residues to produce patterns in three dimensions with specific interparticle distances (Figure 1d and e).[15,16] Viruses decorated with gold nanoparticles (EF with 5 nm particles and DM with 2 nm particles) were exposed to molecules with thiol end groups to produce a conductive network on the virus (Figure 1f and g), which we refer to as a viral nanoblock (VNB). The two molecules chosen for this study, 1,4-C_6H_4[*trans*-(4-$AcSC_6H_4C\equiv CPt(PBu_3)_2C\equiv C]_2$ (di-Pt) and oligophenylenevinylene (OPV), for which detailed *I*/*V* characterization is available,[17–20] are shown in Table 1. Due to the interparticle spacing, the network on the EF mutant (EF-VNB) was formed using both OPV and di-Pt molecules, while the network on the DM mutant (DM-VNB) was formed from OPV alone. Molecular attachment was confirmed with fluorescence spectroscopy,

Table 1. The molecular structure of the molecules used.

Molecule	Molecular structure	Length (nm)
di-Pt	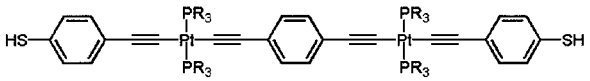	3.04
OPV	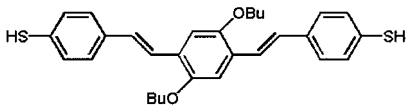	2.07

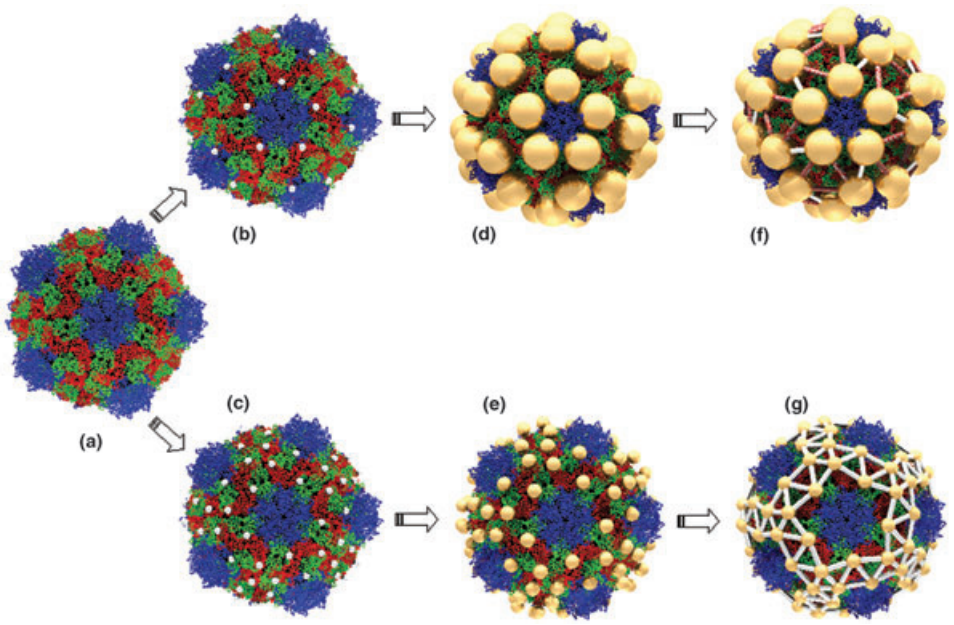

Figure 1. Schematic of the procedure used to create molecular networks on the surface of the virus capsid: a) CPMV capsid structure from crystallographic data; b) EF mutant with one cysteine (white dots) per subunit. The four nearest-neighbor cysteine-to-cysteine distances are 5.3, 6.6, 7.5, and 7.9 nm; c) DM mutant with two cysteines per subunit. The four nearest-neighbor cysteine-to-cysteine distances are 3.2, 4.0, 4.0, and 4.2 nm; d) EF with 5 nm gold nanoparticles bound to the inserted cysteines; e) DM with 2 nm gold nanoparticles bound to the inserted cysteines; f) EF mutant with the 5 nm gold particles interconnected using di-Pt (red) and OPV (silver) molecules; g) DM mutant with the 2 nm gold particles interconnected with OPV molecules.

using the emission of OPV at 457 nm (see Supporting Information, Figure 1).

Although it is possible for the gold–sulfur bond to dissociate or exchange with other thiol compounds, we find that the gold nanoparticles are well-attached to the viral scaffold, and do not detach from the virus in the presence of the molecules. Any weakly bound gold nanoparticles are more likely to be removed by the electric field during electrophoresis for purification or electroelution for recovery.[16] Furthermore, while the location of the cysteines on the capsid determines the positions of the gold nanoparticles, the bound particles are likely stabilized by interactions with the surrounding amino acids of the capsid, as colloidal gold has also been used as a nonspecific protein label for electron microsco-

py,[21] protein immobilization, and electron-transfer experiments.[22]

The conductance of the molecular network self-assembled on a single virus was measured using scanning tunneling microscopy (STM). Even though STM has been used to characterize the conductance of isolated molecules,[19,23–29] this study represents the first measurement of conductance on a self-assembled molecular network on the nanometer scale. To carry out these measurements, a self-assembled monolayer of undecanethiol (C11) on a gold-on-mica substrate was used to isolate VNBs from each other. The dithiol-functionalized conducting molecule OPV (structure shown in Table 1) was inserted into defect sites in the C11 film, producing a number of conductive single molecules that are physically and electronically isolated from each other with a reactive thiol group at the end.[19,23,30,31] This substrate was exposed to VNBs, which resulted in isolated viruses binding to the underlying gold substrate via the inserted conducting molecules, as shown schematically in Figure 2a. C11/OPV films exposed to EF CPMV with attached 5 nm gold nanoparticles show characteristic spotted, darker areas (Figure 2b). These areas do not appear in films that have not been exposed to virus (not shown). These darker areas are 35 ± 2 nm in diameter, which is in good agreement with the virus diameter of 30 nm. Within these darker areas are bright spots that are 5.2 ± 0.6 nm in diameter. We attribute these bright spots to 5 nm gold nanoparticles attached to the virus. Without gold attached, the virus appears as a dark area without the bright spots (image not shown). Figure 2c shows an enlarged STM image of EF viruses with attached gold nanoparticles. Figure 2d shows an STM image of the EF-VNB that has been exposed to conductive molecules prior to insertion in the film. In this image, the bright features on the EF-VNB are highly enhanced and prominent. Although interpreting STM images can be problematic because the image represents a convolution of electronic and topographic information,[23,32] the distinct difference in appearance of the EF-VNBs before and after exposure to conductive molecules suggests that functionalization with molecular wires opened a pathway for charge transport across the network built on the viral scaffold. This is further corroborated by the increase in the measured conductance of the EF-VNBs after exposure to the molecules.

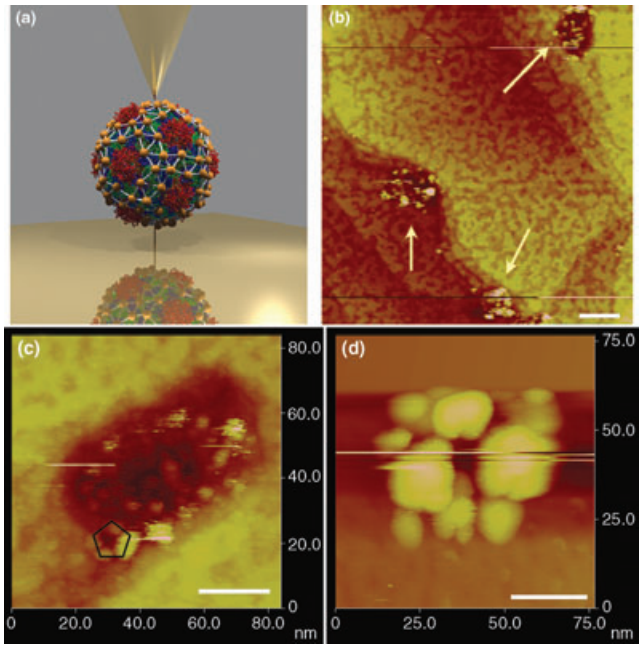

Figure 2. STM studies of viral nanoblocks: a) Schematic of an STM experiment, which shows isolated conductive VNB attached to a gold substrate through a conducting molecule inserted in an insulating C11 matrix; b) STM image showing three EF mutants with 5 nm gold nanoparticles attached in a C11 alkane matrix prior to reaction with molecules. Arrows point to the VNBs. $I_t = 2.5$ pA, $V_{bias} = 1$ V. Scale bar = 20 nm; c) STM image zoomed in on EF mutant with 5 nm gold nanoparticles. The size and shape indicates that there are likely two viruses in this image. Pentagon indicates likely 5-fold axis. Scale bar = 20 nm. d) STM image of EF-conductive VNB in C11 alkane matrix. $I_t = 2.5$ pA, $V_{bias} = 1$ V. Scale bar = 20 nm.

In addition to STM images, tunneling spectroscopy measurements were also made on the viruses to examine the conductance of the molecular networks. For tunneling spectroscopy, the STM tip was held over a particular spot on the surface with the feedback turned off, and then the bias voltage was swept while measuring the tunneling current. Measurements were made on isolated VNBs that showed good coverage on the virus by gold nanoparticles during imaging. Figure 3a shows typical current versus voltage (I/V) curves for EF viruses with (red) and without (blue) the molecular network. These measurements show that the current increased dramatically after the molecules were attached, as suggested by the images in Figure 2c and d. 92% of the VNB particles selected for I/V measurement show this enhancement in the measured tunneling current. Similar measurements made on DM-VNBs also showed a substantial increase in conductance after exposure to molecular wires (Figure 3b). As predicted by simple models of the two molecular networks, DM-VNBs are more conductive than EF-VNBs (see Supporting Information, Figure 2). As a control experiment, we also created EF-VNBs using 2 nm gold nanoparticles instead of 5 nm. Figure 3c shows I/V measurements of EF viruses with 2 nm gold particles attached with (red) and without (blue) bound molecules. In this experiment, there is no difference in the measured conductance, because the attached molecules cannot span the distance between the gold particles. Thus, the presence of the molecules does not change the measured conductance unless a molecular network is formed.

A more detailed HSPICE analysis (circuit simulation program; Synopsis, Inc.) demonstrates the degree of interconnectivity produced on the DM-VNBs. Network A in Figure 4 shows a graphical representation of the full VNB network on the DM mutant identifying four nearest-neighbor distances that can be bridged by the OPV molecule. Analysis was carried out by systematically removing one of these nearest-neighbor connections (Networks B–E in Figure 4), starting with a VNB in which 90% of the cysteines are populated with a gold nanoparticle, out of which 95% of the nearest-neighbor gold nanoparticles are bridged by OPV molecules. This gives a measure of the relative importance of the four different types of nearest-neighbor con-

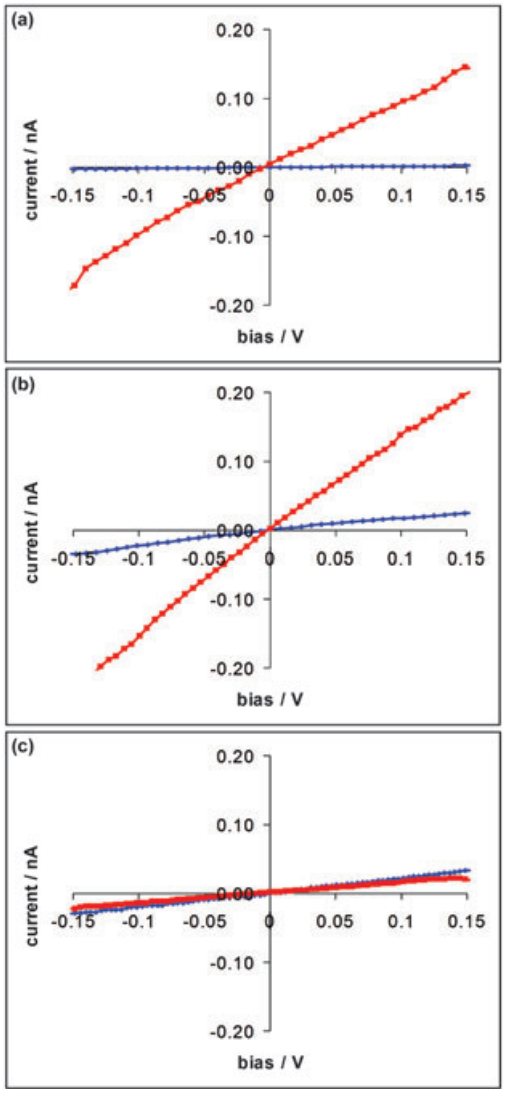

Figure 3. a) Typical *I*/*V* measurements of an EF mutant decorated with 5 nm gold nanoparticles before (blue) and after (red) assembly of OPV and di-Pt molecules. Each curve is an average of 20 measurements; b) Typical *I*/*V* measurements of a DM mutant decorated with 2 nm gold nanoparticles before (blue) and after (red) assembly of OPV molecules. Each curve is an average of 20 measurements (DM-VNBs are 2.3 times more conductive than EF-VNBs); c) Typical *I*/*V* measurements used as negative control of an EF mutant decorated with 2 nm gold nanoparticles before (blue) and after (red) assembly of OPV and di-Pt molecules. Each curve is an average of 20 measurements.

nections. From this model, we see that the red connections are the least important in the formation of the network, such that their removal decreases the network conductance by just 6% to 94% of the maximum. In contrast, the black connections are critical to network formation—if these connections do not form, the overall network conductance is only 17% of the maximum conductance. Figure 4 shows the calculated network conductances for the four models, assuming that an OPV molecule has a conductance of 1. Experimentally, the DM-VNB has a conductance of 0.38 ± 0.15

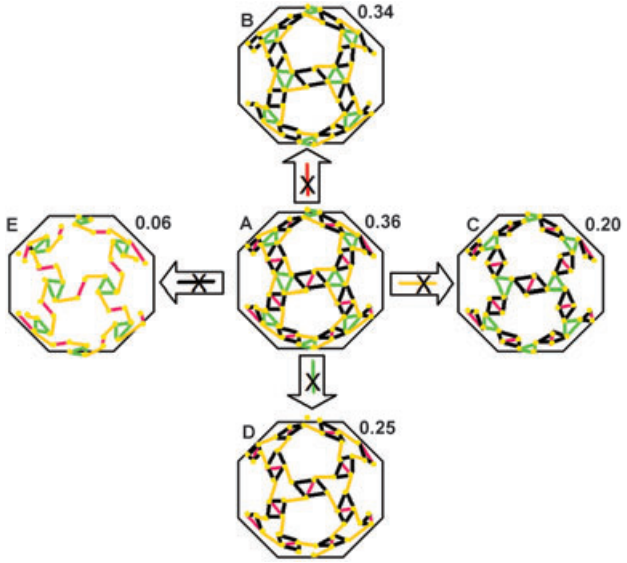

Figure 4. Modeling the DM-VNB network. Calculated conductance based on the number of nearest-neighbor connections, assuming 90% of the gold nanoparticles are present and 95% of the relevant nearest-neighbors are connected. Center model (Network A) has all four nearest-neighbors connected. Each of the four surrounding models (Networks B–E) has one of the connections removed. Numbers in black are the calculated network conductance, assuming a conductance of 1 for each OPV molecule. Experimentally determined conductance is closest to Networks A and B.

normalized to the conductance of a single OPV molecule. This is most consistent with Network A or B, which indicates that molecules are assembling along the critical path for conduction across the virus.

We have successfully used bottom-up self-assembly techniques to produce conductive networks on the nanoscale. Building such electronic circuits from molecular building blocks is an area of much current interest. This bottom-up approach uses different types of molecules for functions such as wires, switches, and diodes, to build electronic circuits, increasing the theoretical device density by up to 10^{14} devices per cm^2.[33] Biological scaffolds hold great promise in assembling and interconnecting novel nanosized components, allowing such organized assemblies to interface with well-developed technologies such as lithography as nanotechnology develops. CPMV, due to its size, monodispersity, and variety of chemical groups available for modification, makes a good scaffold for molecular assembly into nanoscale devices. The CPMV scaffold uses the chemical specificity present in biological systems to organize inorganic components with great precision in three dimensions. Furthermore, CPMV incorporates other reactive chemical groups such as amines and carboxylic acids that can be used to add additional functionality to assemble nanoscale devices in the future. Currently, work is in progress to replace the conductive OPV molecule with molecules that can act as bistable molecular switches.[29] This will enable us to build CPMV-based bit-storage devices with a theoretical density of 10^{15} bits per cm^2.

Keywords:
molecular electronics · nanotechnology · protein engineering · self-assembly · viruses

[1] G. M. Whitesides, B. Grzybowski, *Science* **2002**, *295*, 2418 – 2421.
[2] A. P. Alivisatos, *Nature* **1996**, *382*, 609 – 611.
[3] C. A. Mirkin, R. L. Letsinger, R. C. Mucic, J. J. Storhoff, *Nature* **1996**, *382*, 607 – 609.
[4] M. G. Warner, J. E. Hutchison, *Nat. Mater.* **2003**, *2*, 272 – 277.
[5] R. Elghanian, J. J. Storhoff, R. C. Mucic, R. L. Letsinger, C. A. Mirkin, *Science* **1997**, *277*, 1078 – 1081.
[6] J. J. Storhoff, A. A. Lazarides, R. C. Mucic, C. A. Mirkin, R. L. Letsinger, G. C. Schatz, *J. Am. Chem. Soc.* **2000**, *122*, 4640 – 4650.
[7] S. W. Lee, C. Mao, C. E. Flynn, A. M. Belcher, *Science* **2002**, *296*, 892 – 895.
[8] N. C. Seeman, A. M. Belcher, *Proc. Natl. Acad. Sci. USA* **2002**, *99*, 6451 – 6455.
[9] J. Fang, C. M. Soto, T. Lin, J. E. Johnson, B. Ratna, *Langmuir* **2002**, *18*, 308 – 310.
[10] B. R. Ratna, C. M. Soto, L. Danner, A. S. Blum, J. Fang, T. Lin, J. E. Johnson, *Langmuir* **2003**, *19*, 489 – 490.
[11] T. Lin, Z. Chen, R. Usha, C. V. Stauffacher, J. Dai, T. Schmidt, J. E. Johnson, *Virology* **1999**, *265*, 20 – 35.
[12] T. Lin, C. Porta, G. Lomonossoff, J. E. Johnson, *Folding Des.* **1996**, *1*, 179 – 187.
[13] G. P. Lomonossoff, J. E. Johnson, *Curr. Opin. Struct. Biol.* **1996**, *6*, 176 – 182.
[14] Q. Wang, T. Lin, L. Tang, J. E. Johnson, M. G. Finn, *Angew. Chem.* **2002**, *114*, 477 – 480; *Angew. Chem. Int. Ed.* **2002**, *41*, 459 – 462.
[15] A. S. Blum, C. M. Soto, C. D. Wilson, J. D. Cole, M. Kim, B. Gnade, A. Chatterji, W. F. Ochoa, T. Lin, J. E. Johnson, B. R. Ratna, *Nano Lett.* **2004**, *4*, 867 – 870.
[16] C. M. Soto, A. S. Blum, C. D. Wilson, J. Lazorcik, A. Chatterji, J. E. Johnson, B. R. Ratna, *Electrophoresis* **2004**, *25*, 2901 – 2906.
[17] H. D. Sikes, J. F. Smalley, S. P. Dudek, A. R. Cook, M. D. Newton, C. E. D. Chidsey, S. W. Feldberg, *Science* **2001**, *291*, 1519 – 1523.
[18] J. G. Kushmerick, D. B. Holt, S. K. Pollack, M. A. Ratner, J. C. Yang, T. L. Schull, J. Naciri, M. H. Moore, R. Shashidhar, *J. Am. Chem. Soc.* **2002**, *124*, 10 654 – 10 655.
[19] A. S. Blum, J. C. Yang, R. Shashidhar, B. R. Ratna, *Appl. Phys. Lett.* **2003**, *82*, 3322 – 3324.
[20] T. L. Schull, J. G. Kushmerick, C. H. Patterson, C. George, M. H. Moore, S. K. Pollack, R. Shashidhar, *J. Am. Chem. Soc.* **2003**, *125*, 3202 – 3203.
[21] M. Bendayan, *Biotech. Histochem.* **2000**, *75*, 203 – 242.
[22] S. Q. Liu, D. Leech, H. X. Ju, *Anal. Lett.* **2003**, *36*, 1 – 19.
[23] L. A. Bumm, J. J. Arnold, M. T. Cygan, T. D. Dunbar, T. P. Burgin, L. Jones II, D. L. Allara, J. M. Tour, P. S. Weiss, *Science* **1996**, *271*, 1705 – 1707.
[24] D. I. Gittins, D. Bethell, D. J. Schiffrin, R. J. Nichols, *Nature* **2000**, *408*, 67 – 69.
[25] S. Wakamatsu, U. Akiba, M. Fujihira, *Colloids Surf. A* **2002**, *198–200*, 785 – 790.
[26] W. Haiss, H. van Zalinge, S. J. Higgins, D. Bethell, H. Höbenreich, D. J. Schiffrin, R. J. Nichols, *J. Am. Chem. Soc.* **2003**, *125*, 15 294 – 15 295.
[27] X. Xiao, B. Xu, N. J. Tao, *Nano Lett.* **2004**, *4*, 267 – 271.
[28] A. S. Blum, J. G. Kushmerick, S. K. Pollack, J. C. Yang, M. Moore, J. Naciri, R. Shashidhar, B. R. Ratna, *J. Phys. Chem. B* **2004**, *108*, 18 124 – 18 128.
[29] A. S. Blum, J. G. Kushmerick, D. P. Long, C. H. Patterson, J. C. Yang, J. C. Henderson, Y. Yao, J. M. Tour, R. Shashidhar, B. R. Ratna, *Nat. Mater.* **2005**, *4*, 167 – 172.
[30] M. T. Cygan, T. D. Dunbar, J. J. Arnold, L. A. Bumm, N. F. Shedlock, T. P. Burgin, L. Jones II, D. L. Allara, J. M. Tour, P. S. Weiss, *J. Am. Chem. Soc.* **1998**, *120*, 2721 – 2732.
[31] X. D. Cui, A. Primak, X. Zarate, J. Tomfohr, O. F. Sankey, A. L. Moore, T. A. Moore, D. Gust, G. Harris, S. M. Lindsay, *Science* **2001**, *294*, 571 – 574.
[32] R. Wiesendanger, *Scanning Probe Microscopy and Spectroscopy*, Cambridge University Press, Cambridge, **1994**.
[33] M. A. Reed, J. M. Tour, *Sci. Am.* **2000**, *282*, 86 – 93.

Received: January 18, 2005

